

# Double D- $\pi$ -A Dye Linked by 2,2'-Bipyridine Dicarboxylic Acid: Influence of *para*- and *meta*-Substituted Carboxyl Anchoring Group

Paramaguru Ganesan,<sup>[a, b]</sup> Aravind Kumar Chandiran,<sup>[a, c]</sup> Peng Gao,<sup>\*[a]</sup> Renganathan Rajalingam,<sup>[b]</sup> Michael Grätzel,<sup>[a]</sup> and Mohammad Khaja Nazeeruddin<sup>\*[a]</sup>

Starting from 2,2'-bipyridine dicarboxylic acid, two new (D- $\pi$ -A)<sub>2</sub> sensitizers, including *m*-DA with the carboxyl anchoring group substituted *meta* to the donor-bridge moiety and *p*-DA with a *para*-substituted anchoring group, were synthesized in order to evaluate the impact of the position of the anchoring group on the optical, electrochemical, and photovoltaic properties of dye-sensitized solar cells. *p*-DA exhibits red-shifted absorption behavior compared to *m*-DA, owing to the more efficiently extended  $\pi$ -conjugation with *para* substitution. Both *m*-DA and *p*-DA are adsorbed on the mesoporous TiO<sub>2</sub> surface by using both of their carboxylic acid groups in a banchoring mode, which is confirmed through attenuated total reflectance

FTIR analysis. Red-shifted absorption of *p*-DA assists the achievement of a red-shifted incident photon-to-electron conversion efficiency and a higher short-circuit current density than *m*-DA. The photogenerated electron lifetime in TiO<sub>2</sub> is also found to be higher for *para* substituted *p*-DA than the *meta*-substituted *m*-DA, which results in a higher open-circuit voltage. All of the results suggest that dicarboxyl-2,2'-bipyridine can be used as an acceptor for metal-free organic sensitizers. However, the anchoring segments should be adjusted to the favorable position of the corresponding donor-bridge moieties for better conjugation.

## 1. Introduction

Dye-sensitized solar cells (DSSC), commonly known as Grätzel cells, have emerged as a promising solar energy-conversion technology to meet the energy demand of the future.<sup>[1,2]</sup> DSSCs have received great attention from both academia and industry, owing to their low cost and easy fabrication methods. Among the different components determining the performance of DSSCs, sensitizers that harvest solar radiation play a key role in achieving high efficiencies. So far, ruthenium-based complexes and zinc-porphyrin sensitizers show promising photovoltaic power conversion efficiencies (PCE) of 11 and 13%, respectively.<sup>[3-5]</sup> Owing to the rare availability, high cost, and low molar extinction coefficient of ruthenium-based sensitizers, quests to develop organic-based sensitizers have been

receiving increasing attention in recent years. With many approaches to different organic sensitizers, the most effective structural arrangement of an organic dye consists of donor and acceptor groups bridged through a  $\pi$  spacer (D- $\pi$ -A).<sup>[6]</sup> Recently, Grätzel et al. achieved a record PCE of 10.65% with a single D- $\pi$ -A organic molecule, which motivated researchers to further develop new efficient sensitizers, sustaining important factors such as broad absorption in the visible region, strong binding affinity with TiO<sub>2</sub>, good electron injection, good stability, and cost effectiveness.<sup>[7]</sup> The development of substituted multianchor dyes has been getting great attention in recent years to enhance the binding strength and electron injection efficiency.<sup>[8]</sup> The most common strategy is that a donor and  $\pi$  spacer are attached to anchoring groups with two acceptors (D- $\pi$ -A<sub>2</sub>),<sup>[9]</sup> and there are a few reports focused on using the double donor- $\pi$ -acceptor approach (D- $\pi$ -A)<sub>2</sub>.<sup>[10]</sup> In both of these strategies, despite the change in choices of donor and  $\pi$  spacer groups, cyanoacrylic acid is the most widely used acceptor and anchoring moiety. This is evident from the recent review of multianchoring groups, where all the dyes have cyanoacrylic acid as the anchoring moiety.<sup>[11]</sup> Kloo et al. and Sun et al. observed the problem of photoisomerization and degradation of cyanoacrylic acid, which will affect the dye performance in the long term.<sup>[12]</sup> When multiple cyanoacrylic acids are employed in one molecule, the problem will become more complicated. Therefore, we have tried to overcome this situation by using carboxylic acids as anchoring groups, like ruthenium dye counterparts.

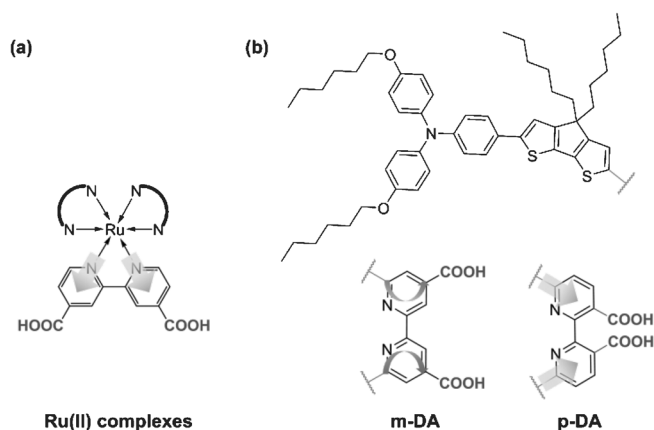
[a] Dr. P. Ganesan, Dr. A. K. Chandiran, Dr. P. Gao, Prof. Dr. M. Grätzel, Prof. M. K. Nazeeruddin  
Laboratory for Photonics and Interfaces  
Institute of Chemical Sciences and Engineering  
Ecole Polytechnique Fédérale de Lausanne  
CH-1015 Lausanne (Switzerland)  
E-mail: peng.gao@epfl.ch  
mdkhaja.nazeeruddin@epfl.ch

[b] Dr. P. Ganesan, Prof. R. Rajalingam  
School of Chemistry, Bharathidasan University  
Tiruchirappalli 620024, Tamilnadu (India)

[c] Dr. A. K. Chandiran  
Current address:  
Department of Chemistry  
University of California, Berkeley, CA, 94720-1460 (USA)

Supporting Information for this article is available on the WWW under <http://dx.doi.org/10.1002/cphc.201402822>.

Based on the above discussion, we attempted to use two different kinds of 2,2'-bipyridine dicarboxylic acids to develop new types of (D- $\pi$ -A)<sub>2</sub> sensitizers. 2,2'-Bipyridine dicarboxylic acids, which are commonly used in ruthenium dyes, were chosen because of their flexible structural arrangement in coupling two donors and the inherent two-carboxyl-acceptor part. (Scheme 1) To the best of our knowledge, this is the first



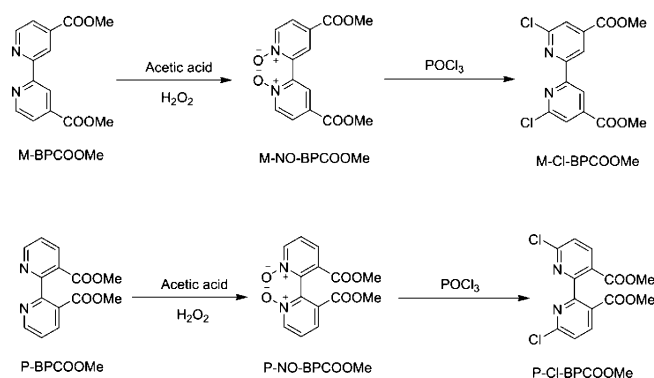
**Scheme 1.** a) Chemical structure of commonly employed ruthenium complexes containing carboxyl anchoring groups. b) Chemical structure of the (D- $\pi$ -A)<sub>2</sub> sensitizers with carboxyl anchoring groups that attached to the donor segment in the *para* or *meta* positions.

report in which bipyridine acceptors are used in organic sensitizers. In the two sensitizers that we designed and synthesized, carboxylic acids were attached to 2,2'-bipyridine with two different situations, that is, *m*-DA with the anchoring part substituted *meta* to the donor part and *p*-DA with a *para*-substituted anchoring part. The two new sensitizers were fully characterized by NMR, mass techniques, UV/Vis absorption, photoluminescence (PL), and cyclic voltammetry (CV). The impact of the position of the anchoring part on the optical, electrochemical and photovoltaic properties was also investigated.

## 2. Results and Discussion

### 2.1. Synthesis and Characterization of *m*-DA and *p*-DA

The 2,2'-bipyridine-based acceptors with carboxyl groups at different positions were synthesized, and the synthetic routes are depicted in Scheme 2. The donor- $\pi$ -spacer **1** was synthesized by employing the previously reported procedure and then converted to its stannous analogue for convenient coupling with the acceptor fragments to give the methyl carboxyl-

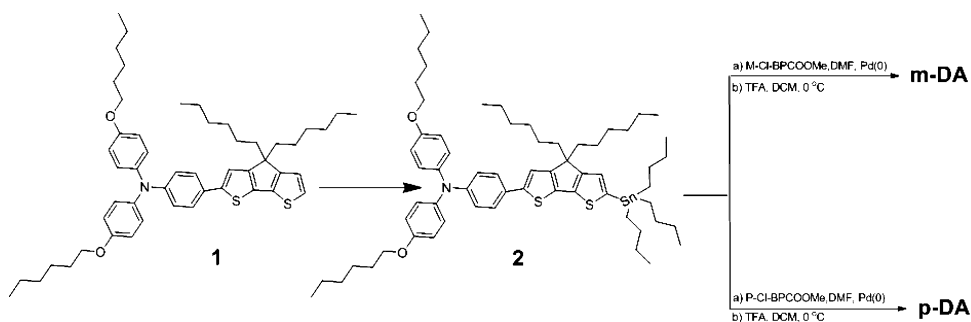


**Scheme 2.** Synthetic route employed for 2,2'-bipyridine-based acceptor with carboxyl groups at different positions.

ate precursors.<sup>[13]</sup> Hydrolysis of these precursors by using LiOH afforded the final sensitizers *m*-DA and *p*-DA. (Scheme 3) All intermediates and the final compounds were characterized by <sup>1</sup>H NMR, <sup>13</sup>C NMR, and mass spectroscopy. The observed NMR and mass data correlated well with the expected final compounds.

### 2.2. Optical and Electrochemical Properties

The influence of *para*- and *meta*-substituted carboxyl anchoring groups on the light-harvesting properties of the sensitizers was scrutinized by using ground-state absorption measurements. It can be seen from the absorption spectra of *m*-DA



**Scheme 3.** Synthetic route employed for final (D- $\pi$ -A)<sub>2</sub> sensitizers *m*-DA and *p*-DA.

and *p*-DA that the change in positions of the carboxyl anchoring group affects the absorption spectra of the dyes. (Figure 1A) The *meta*-substituted -COOH dye (*m*-DA) exhibits a major absorption band from 370 to 525 nm with a maximum around 471 nm. When the -COOH group is present in the *para* position, there is a 7 nm redshift in the maximum absorption and the absorption edge experiences a greater redshift and appears around 555 nm. This phenomenon is attributed to the possibility of  $\pi$ -conjugation shifts towards the carboxylic group in *p*-DA, owing to the substitution in *para* position and results in prominent charge-transfer (CT) transition. However, owing to the *meta*-positioned -COOH group in *m*-DA, the extended conjugation is not overlapped with the -COOH moiety and results in a CT band. Furthermore, the molar extinction co-

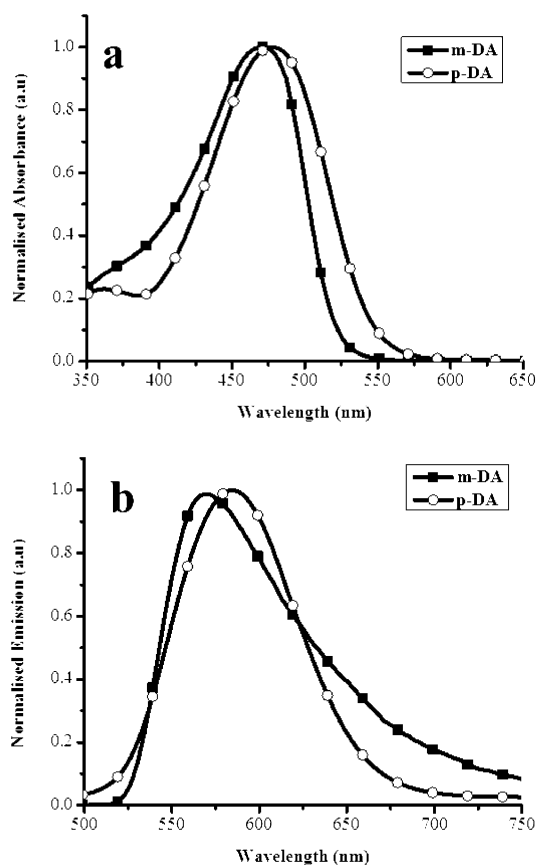


**Figure 1.** a) Absorption and b) emission spectra of sensitizers *m*-DA and *p*-DA in dichloromethane ( $1 \times 10^{-5}$  M).

efficient of *p*-DA is found to be higher than *m*-DA. The emission behavior of both dyes excited at their absorption maximum wavelength was recorded in dichloromethane solution and the spectra are displayed in Figure 1B. *m*-DA and *p*-DA have maximum emissions at 569 and 584 nm, respectively. Similar to their absorption behavior, the maximum emission wavelength of *p*-DA is red-shifted by 15 nm compared to that of *m*-DA.

Energy levels of sensitizers are imperative parameters to determine the ability of electron injection from the excited dye molecules to the conduction band (CB) of  $\text{TiO}_2$  and dye regeneration through the redox couple. CV was carried out to measure and understand the impact of the positions of the anchoring groups on the oxidation potential of the sensitizers. Figure 2a displays the CV traces of both dyes, in which two oxidation peaks are observed. The first redox process (HOMO) (0.77 V vs. NHE for *m*-DA and 0.74 V vs. NHE for *p*-DA) occurs because of the presence of a triphenyl amine segment, as observed from earlier reports, which are more positive than the redox potential of the  $\text{I}^-/\text{I}_3^-$  redox couple ( $\approx 0.4$  V vs. NHE),<sup>[14]</sup> implying the thermodynamic feasibility of regeneration of the oxidized dyes. Correspondingly, the excited-state oxidation potential of the dyes (LUMO) will give information about their electron-injection possibilities to the CB of  $\text{TiO}_2$ . The LUMO levels of the dyes were calculated from the difference between the HOMO level and the band-gap energy. The band gap ( $E_{0-0}$ )

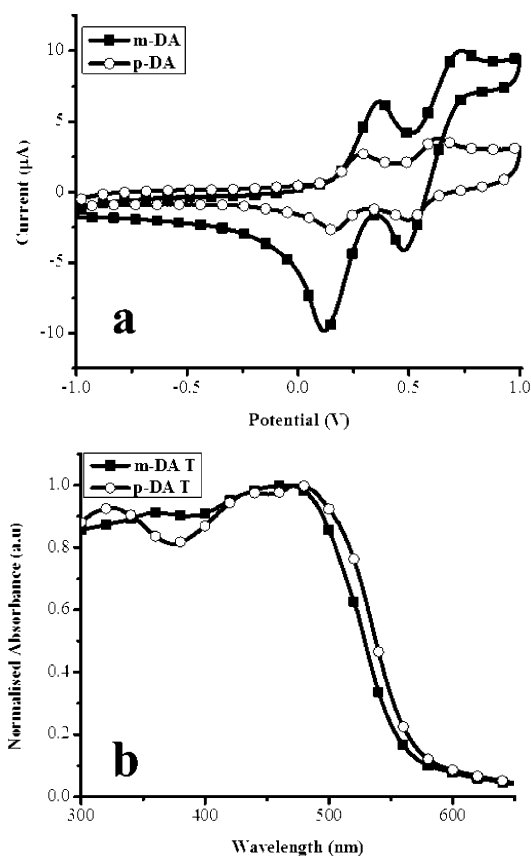


**Figure 2.** a) Cyclic voltammogram of *m*-DA and *p*-DA. b) Absorption spectrum of sensitizers *m*-DA and *p*-DA adsorbed on  $\text{TiO}_2$  film.

was estimated from the intersection of the normalized absorption and emission spectra. The LUMO levels of *m*-DA and *p*-DA were calculated to be around  $-1.59$  V versus NHE and  $-1.58$  V versus NHE, respectively, which are more negative than the conduction-band edge of  $\text{TiO}_2$  electrode ( $-0.5$  V vs. NHE),<sup>[15]</sup> implying that these dyes can efficiently inject an electron from their excited states to the CB of  $\text{TiO}_2$ . It is worth noting that there is considerable difference in the second oxidation process of both sensitizers, which may be attributed to the variation of the positions of substituted anchoring groups. All data are detailed in Table 1.

**Table 1.** Photophysical and electrochemical properties of sensitizers *m*-DA and *p*-DA.

Sensitizer	Absorption $\lambda_{\text{max}}$ <sup>[a]</sup> [nm]	Emission $\lambda_{\text{max}}$ <sup>[a]</sup> [nm]	HOMO <sup>[b]</sup> [V vs. NHE]	Band gap <sup>[c]</sup> [eV]	LUMO <sup>[d]</sup> [V vs. NHE]
<i>m</i> -DA	471	569	0.77	2.36	$-1.59$
<i>p</i> -DA	478	584	0.74	2.32	$-1.58$

[a] Absorption or emission maximum in dichloromethane solution. [b] The HOMO was taken from the first redox potential in CV plot. Potentials measured versus  $\text{Fc}^+/\text{Fc}$  were converted to normal hydrogen electrode (NHE) by adding  $+0.63$  V. [c] The band gap ( $E_{0-0}$ ) was estimated from the intersection of the normalized absorption and emission spectra. [d] The LUMO was calculated with the expression of  $\text{LUMO} = \text{HOMO} - \text{Band Gap}$ .

### 2.3. Binding Properties of *m*-DA and *p*-DA with TiO<sub>2</sub>

To analyze the binding behavior of the dyes on the TiO<sub>2</sub> surface, the absorption spectra of the two sensitizers loaded on a TiO<sub>2</sub> film (5 μm in thickness) were measured and the results are displayed in Figure 2b. Both dyes have similar maximum absorption wavelengths compared to their solution-state absorption spectra, whereas their absorption edges appeared around 561 and 573 nm for *m*-DA-T and *p*-DA-T, respectively, which are red-shifted by 36 and 18 nm, indicating the *J*-aggregation of the dye molecules upon binding with the TiO<sub>2</sub> surface.<sup>[16]</sup> Attenuated total reflectance FTIR (ATR-FTIR) spectroscopy has been widely utilized to probe the interactions between the carboxylic acid groups and the TiO<sub>2</sub> surface. Figure 3

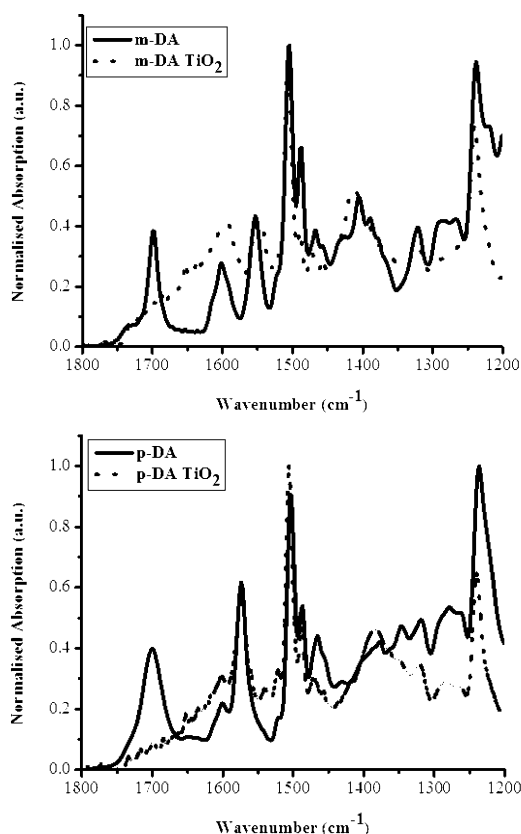


**Figure 3.** FTIR spectra of *m*-DA and *p*-DA in the solid state and the dyes adsorbed on TiO<sub>2</sub> films.

shows the ATR-FTIR spectra of the dyes on glasses or adsorbed on the TiO<sub>2</sub> surface. On a glass substrate, both *m*-DA and *p*-DA showed a strong absorption signal around 1699 cm<sup>-1</sup>, which is attributed to the C=O stretching frequency of free carboxylic acid group (black line). Upon binding with the TiO<sub>2</sub> surface, this signal completely disappears, as seen in the FTIR spectra (grey line). The complete disappearance of the free carboxylic acid group indicates that both *m*-DA and *p*-DA are adsorbed on the TiO<sub>2</sub> surface by using both of their carboxylic acid groups in a so called “bidentate chelate mode”. These observations are well corroborated by the previously reported IR characteristics of sensitizers with carboxylic acid anchoring groups.<sup>[17]</sup>

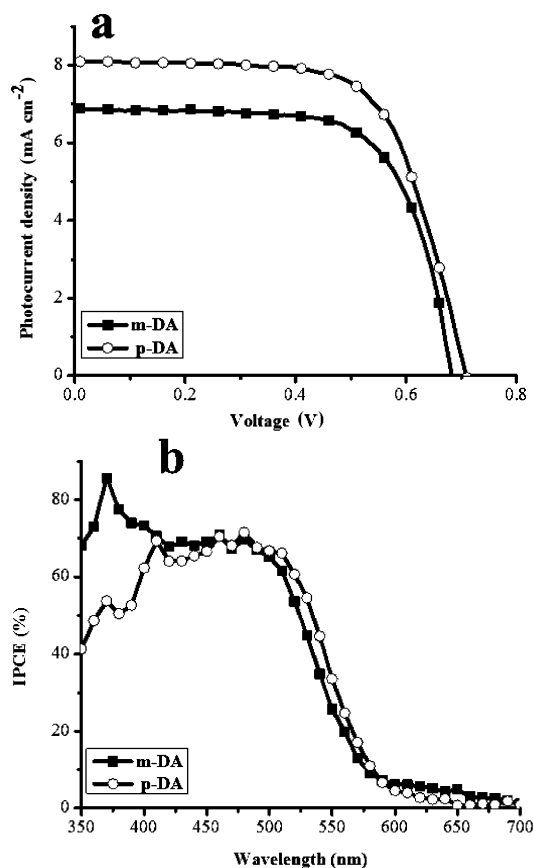


**Figure 4.** a) Current–voltage characteristics measured under simulated AM 1.5 G simulated sunlight (100 mW cm<sup>-2</sup>) for devices employing *m*-DA and *p*-DA. b) IPCE spectra of sensitizers *m*-DA and *p*-DA.

### 2.4. Photovoltaic Properties of *m*-DA and *p*-DA

DSSC devices were fabricated with these dyes to evaluate the influence of two different types of substitution on the PCEs. The DSSCs were all measured under simulated one-sun illumination (AM 1.5 G irradiation at 100 mW cm<sup>-2</sup>). The photocurrent density voltage (*J*-*V*) curves are shown in Figure 4 and the corresponding photovoltaic data are listed in Table 2. It is interesting to look over the short-circuit current density (*J*<sub>sc</sub>), owing to the distinct feature in the direction of orientation for electron injection. *m*-DA with *meta*-substituted anchoring groups produces 7.01 mA cm<sup>-2</sup>, whereas the *J*<sub>sc</sub> of *p*-DA increased by 1.18 mA cm<sup>-2</sup> to reach 8.19 mA cm<sup>-2</sup>. The observed difference

Table 2. Photovoltaic performance of DSSCs of <i>m</i> -DA and <i>p</i> -DA using iodide/triiodide redox mediator. <sup>[a]</sup>				
Cells	<i>V</i> <sub>oc</sub> [V]	<i>J</i> <sub>sc</sub> [mA cm <sup>-2</sup> ]	FF	<i>η</i> [%]
<i>m</i> -DA	0.682	7.01	0.69	3.3
<i>p</i> -DA	0.708	8.19	0.67	3.9

[a] TiO<sub>2</sub> film has a 8 μm scattering layer and a 5 μm transparent layer. Electrolyte composition: 1.0 M DMII (1,3-dimethylimidazolium iodide), 0.03 M iodine, 0.025 M NaI, 0.5 TBP, 0.1 M guanidinium thiocyanide, and acetonitrile solvent.

in  $J_{SC}$  values indicates a more efficient electron injection from the LUMO of the dye molecule to the CB of  $\text{TiO}_2$  through the *para*-substituted anchoring group compared with the *meta*-substituted anchoring group. Similarly, the open-circuit voltage ( $V_{OC}$ ) of *p*-DA was 26 mV greater than *m*-DA, whereas the fill factors (FFs) of these two dyes were almost the same. Owing to the higher  $J_{SC}$  and  $V_{OC}$  values with *p*-DA, its overall conversion efficiency reached 3.9% compared to 3.3% for *m*-DA. Incident photon-to-current conversion efficiency (IPCE) measurements can provide a clear picture of the ability of the sensitizers to convert the absorbed light energy into a current. The photocurrent response spectra of all sensitizers were measured with their corresponding photovoltaic devices, and the plots of IPCE as a function of wavelength are displayed in Figure 4B. *p*-DA shows slightly red-shifted IPCE compared to *m*-DA, which is in line with their absorption behavior. This small red-shifted IPCE contributes to the higher current of *p*-DA. Both dyes have approximately 60% IPCE in the 400–520 nm regions.

The reason for the difference in  $J_{SC}$  values is well supported by their absorption and IPCE measurements. The  $V_{OC}$  difference is mainly governed either by the distribution of trap states below the CB on the semiconductor or by the recombination of the injected electrons from the  $\text{TiO}_2$  to the redox species. Charge extraction measurements were carried out to analyze the trap states of the dye-sensitized  $\text{TiO}_2$  surface. Figure 5a represents the photovoltage as a function of capacitance. The observed results suggest that both types of anchoring position have a similar type of trap states. Hence, transient photovoltage decay measurements were carried out to analyze the recombination of electrons injected in the  $\text{TiO}_2$  through reductive electron transfer to the electrolyte, and a lower recombination process results in a longer lifetime of the electron. As displayed in Figure 5b, at a given capacitance, the electron lifetime of *p*-DA is longer than *m*-DA, which resulted in a 26 mV higher  $V_{OC}$  than *p*-DA. The possible reason for the difference in recombination rate is attributed to the effective conjugation of the *para*-substituted anchoring group with  $\text{TiO}_2$  in *p*-DA, which injects electrons deep in the  $\text{TiO}_2$  surface for better electron percolation. Because there is no effective conjugation for *m*-DA with  $\text{TiO}_2$ , it injects only to the surface of the semiconductor and enhances the recombination process. This elucidation is well supported by the observation of Wiberg et al. for the different recombination rates between a well-conjugated cyanoacrylic acid anchoring group and less-conjugated rhodanine acetic acid anchoring group.<sup>[18]</sup>

### 3. Conclusions

For the first time, two new (D- $\pi$ -A)<sub>2</sub> organic sensitizers (*m*-DA, *p*-DA) employing a 2,2'-bipyridine dicarboxylic acid unit as an acceptor and anchoring group were designed. *m*-DA has the anchoring part substituted *meta* to the donor moiety and *p*-DA has a *para*-substituted anchoring part. The two new dyes were successfully synthesized and characterized by using NMR and mass spectroscopy. The impacts of the different anchoring-group substitution on optical, electrochemical, and photovoltaic properties were investigated. Red-shifted absorption

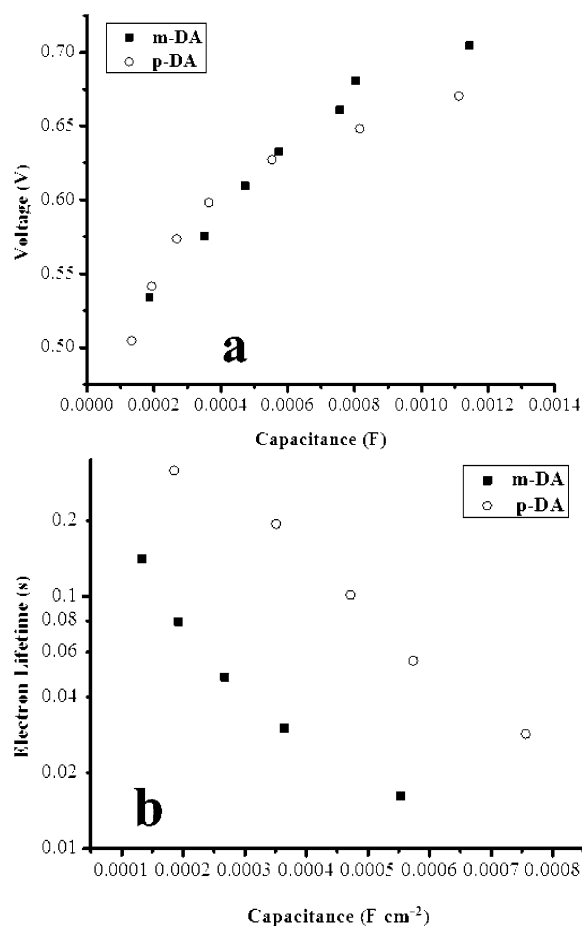


**Figure 5.** a) Distribution of trap state and b) electron lifetimes as a function of capacitance, as measured by using transient photocurrent and photovoltage decay techniques for devices made with *m*-DA and *p*-DA.

behavior was observed for the *para*-substituted *p*-DA compared to *m*-DA. Analysis from ATR-FTIR measurements confirmed that both *m*-DA and *p*-DA were adsorbed on the  $\text{TiO}_2$  surface by using both of their carboxylic acid groups in a biantichoring mode. Owing to the red-shifted absorption of *p*-DA, its  $J_{SC}$  is higher than *m*-DA, which is again reflected in the slightly broadened IPCE of *p*-DA. As probed from transient measurements, the reason for the 26 mV higher  $V_{OC}$  of *p*-DA compared to that of *m*-DA is the difference in their charge recombination rate or electron lifetime. Overall the *para*-substituted dye exhibited better photovoltaic performance than *m*-DA. The observed results provide vital information for the future design of double-acceptor-based sensitizers with better efficiencies.

### Experimental Section

#### Synthesis of *p*-DA-COOMe

To a 100 mL flame-dried,  $\text{N}_2$ -filled round-bottomed flask charged with a stirrer bar, we added *p*-Cl-BP-COOMe (0.040 g) and 4-(4,4-dihexyl-6-(tributylstannyl)-4H-cyclopenta[1,2-b:5,4-b'] dithiophen-2-yl)-N,N-bis(4-hexyloxy)phenyl)aniline 6 (485 mg).  $\text{Pd}(\text{PPh}_3)_4$  (100 mg) was then added, followed by a freeze-pump-thaw degassing process. Anhydrous DMF (20 mL) was then added and the reaction mixture was heated to 80 °C for 12 h. Dichloromethane (50 mL)

was added to the reaction mixture, which was subsequently washed with saturated sodium chloride aqueous solution (3 × 75 mL) and then with water (3 × 75 mL). The organic layer was separated and dried over magnesium sulfate. After removal of the solvent, the crude mixture was purified with gradient silica gel chromatography: 100:0 to 50:50 (hexane/DCM) to give *p*-DA-COOme (0.13 g, 36%) as a red-colored semisolid. <sup>1</sup>H NMR (400 MHz, CDCl<sub>3</sub>): δ = 8.31–8.19 (m, *J* = 8.2 Hz, 2H), 7.72–7.63 (m, *J* = 8.5 Hz, 2H), 7.55 (s, 2H), 7.49–7.40 (m, 4H), 7.20–6.99 (m, 10H), 6.95 (d, *J* = 8.9 Hz, 4H), 6.89–6.84 (m, 8H), 3.97 (t, *J* = 6.5 Hz, 8H), 3.75 (s, 6H), 1.85–1.79 (m, 8H), 1.53–1.47 (m, 8H), 1.39 (td, *J* = 3.7, 7.3 Hz, 20H), 1.34–1.31 (m, 8H), 1.22–1.16 (m, 20H), 0.97–0.92 (m, 20H), 0.84 ppm (t, *J* = 6.8 Hz, 12H); <sup>13</sup>C NMR (100 MHz, CDCl<sub>3</sub>): δ = 167.4, 160.3, 158.3, 158.1, 155.5, 154.2, 148.2, 146.6, 143.0, 141.6, 140.4, 138.5, 137.6, 134.6, 130.6, 127.1, 126.5, 125.9, 123.5, 120.7, 120.7, 118.6, 116.4, 116.2, 115.3, 68.3, 54.0, 52.3, 38.0, 31.6, 31.6, 29.7, 29.5, 29.3, 27.8, 26.9, 26.8, 25.7, 24.5, 22.6, 22.6, 19.6, 17.5, 14.1, 14.0, 13.6 ppm.

### Synthesis of *p*-DA

To a 50 mL round-bottomed flask, we added *p*-DA-COOme (0.1 g) and THF (30 mL). The mixture was cooled to 0 °C and 2 M LiOH (30 mL) was added slowly and the reaction mixture was stirred for about 24 h. Dichloromethane (50 mL) was added to the reaction mixture, which was subsequently washed with acetic acid solution (3 × 75 mL) and then with water (3 × 75 mL). The organic layer was separated and dried over magnesium sulfate. After removal of the solvent, the crude mixture was purified with gradient silica gel chromatography using DCM/methanol/acetic acid (0.8:0.1:0.1) as a final eluent to yield *p*-DA (0.06 g, 36%) as a red-colored semisolid. m.p. 246–248 °C; <sup>1</sup>H NMR (400 MHz, CDCl<sub>3</sub>): δ = 8.39 (br. s., 1H), 7.71 (d, *J* = 8.5 Hz, 2H), 7.55 (s, 2H), 7.44 (d, *J* = 8.5 Hz, 4H), 7.28–6.98 (m, 11H), 6.95 (d, *J* = 8.9 Hz, 4H), 6.89–6.82 (m, 8H), 3.97 (t, *J* = 6.7 Hz, 8H), 2.38–2.31 (m, 4H), 1.82–1.80 (m, 4H), 1.67–1.57 (m, 8H), 1.37 (td, *J* = 3.6, 7.4 Hz, 20H), 1.33–1.31 (m, 9H), 1.23–1.18 (m, 21H), 0.95–0.90 (m, 20H), 0.84 ppm (s, 12H); <sup>13</sup>C NMR (101 MHz, CDCl<sub>3</sub>): δ = 179.4, 158.3, 155.6, 148.3, 140.4, 130.1, 130.0, 129.8, 127.9, 127.0, 126.6, 126.0, 120.6, 116.2, 115.3, 68.3, 54.1, 38.0, 34.0, 32.0, 31.7, 31.6, 31.6, 29.8, 29.8, 29.7, 29.7, 29.6, 29.5, 29.5, 29.4, 29.4, 29.3, 29.2, 29.1, 27.2, 27.0, 25.8, 24.7, 24.6, 22.7, 22.7, 22.6, 14.1, 14.1, 13.6 ppm; HRMS (MALDI) *m/z*: calcd for C<sub>114</sub>H<sub>138</sub>N<sub>4</sub>O<sub>8</sub>S<sub>4</sub>: 1818.9398 [M]<sup>+</sup>; found 1818.9828; elemental analysis calcd (%): C 75.21, H 7.64; found: C 75.26, H 7.61.

### Synthesis of *m*-DA-COOme

A similar method to that for the synthesis of *p*-DA-COOme was applied to give *m*-DA-COOme (0.1 g, 30%) as a red-colored solid. <sup>1</sup>H NMR (400 MHz, CD<sub>2</sub>Cl<sub>2</sub>): δ = 8.76 (s, 1H), 8.03 (s, 1H), 7.58 (s, 1H), 7.51 (d, *J* = 8.6 Hz, 3H), 7.11 (d, *J* = 7.6 Hz, 6H), 6.90 (d, *J* = 8.8 Hz, 9H), 4.06 (s, 4H), 3.99 (t, *J* = 6.5 Hz, 6H), 2.12–2.01 (m, 6H), 1.83 (dt, *J* = 14.5, 6.6 Hz, 6H), 1.74–1.65 (m, 5H), 1.57–1.47 (m, 8H), 1.45–1.21 (m, 42H), 1.15 (s, 6H), 0.98 (t, *J* = 7.3 Hz, 16H), 0.87 ppm (t, *J* = 6.8 Hz, 9H); <sup>13</sup>C NMR (101 MHz, CD<sub>2</sub>Cl<sub>2</sub>): δ = 165.62, 160.08, 155.82, 155.32, 146.44, 139.14, 126.78, 125.77, 120.34, 117.55, 115.24, 68.30, 38.34, 31.65, 29.91, 29.35, 27.86, 26.86, 25.76, 22.67, 17.48, 13.87, 13.41 ppm.

### Synthesis of *m*-DA

A similar method to that for the synthesis of *p*-DA was applied to give *m*-DA (0.12 g, 35%) as a red-colored solid. m.p. 224–228 °C;

<sup>1</sup>H NMR (400 MHz, [D<sub>8</sub>]THF): δ = 13.31 (s, 3H), 8.88 (s, 1H), 8.33 (s, 1H), 7.83 (s, 1H), 7.46 (d, *J* = 8.8 Hz, 3H), 7.26 (s, 1H), 7.03 (d, *J* = 9.0 Hz, 6H), 6.87 (dd, *J* = 22.9, 8.8 Hz, 10H), 3.94 (t, *J* = 6.4 Hz, 6H), 3.58 (s, 18H), 2.20 (s, 2H), 2.01 (d, *J* = 7.8 Hz, 7H), 1.75 (d, *J* = 16.8 Hz, 33H), 1.55–1.45 (m, 8H), 1.39 ppm (d, *J* = 9.0 Hz, 19H); <sup>13</sup>C NMR (101 MHz, THF) δ = 160.00, 157.97, 155.77, 148.23, 146.40, 143.78, 140.39, 136.95, 134.52, 127.94, 127.09, 126.41, 125.64, 125.01, 120.39, 116.15, 115.03, 67.89, 67.39, 41.15, 38.01, 34.11, 31.60, 29.82, 29.31, 25.74, 24.59, 24.39, 24.17, 22.56, 20.55, 13.54, 13.52 ppm; HRMS (MALDI) *m/z*: calcd for C<sub>114</sub>H<sub>138</sub>N<sub>4</sub>O<sub>8</sub>S<sub>4</sub>: 1820.6180 [M]<sup>+</sup>; found 1819.9087; elemental analysis calcd (%): C 75.21, H 7.64; found: C 75.23, H 7.62.

### Acknowledgements

R.R. thanks the Department of Science and Technology (DST) (reference number SR/S1/PC-12/2011, DT: 20.09.2011) for the project. G.P. thanks the Swiss Government Scholarship (Ref No: 2012.0795/India/OP.) P.G. thanks the European Community's Seventh Framework Programme (FP7/2007-2013) ENERGY.2012.10.2.1; NANOMATCELL, grant agreement no. 308997K. M.K.N. acknowledges the World Class University programme, Photovoltaic Materials, Department of Material Chemistry, Korea University, Chungnam, Korea, funded by the Ministry of Education, Science and Technology through the National Research Foundation of Korea (no. R31-2008-000-10035-0).

**Keywords:** 2,2'-bipyridine · bianchoring · double acceptor · dyes/pigments · solar cells

- [1] B. O'Regan, M. Grätzel, *Nature* **1991**, *353*, 737–740.
- [2] M. Grätzel, *Nature* **2001**, *414*, 338–344.
- [3] a) M. Grätzel, *J. Photochem. Photobiol. A* **2004**, *164*, 3–14; b) M. K. Nazeeruddin, A. Kay, I. Rodicio, R. Humphry-Baker, E. Mueller, P. Liska, N. Vlachopoulos, M. Graetzel, *J. Am. Chem. Soc.* **1993**, *115*, 6382–6390; c) M. K. Nazeeruddin, R. Splivallo, P. Liska, P. Comte, M. Grätzel, *Chem. Commun.* **2003**, 1456–1457; d) P. Wang, S. M. Zakeeruddin, I. Exnar, M. Grätzel, *Chem. Commun.* **2002**, 2972–2973; e) P. Wang, S. M. Zakeeruddin, J. E. Moser, M. K. Nazeeruddin, T. Sekiguchi, M. Grätzel, *Nat. Mater.* **2003**, *2*, 402–407.
- [4] a) A. Yella, H. W. Lee, H. N. Tsao, C. Yi, A. K. Chandiran, M. K. Nazeeruddin, E. W. G. Diau, C. Y. Yeh, S. M. Zakeeruddin, M. Grätzel, *Science* **2011**, *334*, 629–634; b) S. Mathew, A. Yella, P. Gao, R. Humphry-Baker, B. F. E. Curchod, N. Ashari-Astani, I. Tavernelli, U. Rothlisberger, M. K. Nazeeruddin, M. Grätzel, *Nat. Chem.* **2014**, *6*, 242–247.
- [5] a) R. Chen, X. Yang, H. Tian, L. Sun, *J. Photochem. Photobiol. A* **2007**, *189*, 295–300; b) R. Chen, X. Yang, H. Tian, X. Wang, A. Hagfeldt, L. Sun, *Chem. Mater.* **2007**, *19*, 4007–4015; c) Y. Hao, X. Yang, J. Cong, H. Tian, A. Hagfeldt, L. Sun, *Chem. Commun.* **2009**, 4031–4033.
- [6] a) N. Hirata, J.-J. Lagref, E. J. Palomares, J. R. Durrant, M. K. Nazeeruddin, M. Grätzel, D. Di Censo, *Chem. Eur. J.* **2004**, *10*, 595–602; b) J. N. Clifford, E. Palomares, M. K. Nazeeruddin, M. Grätzel, J. Nelson, X. Li, N. J. Long, J. R. Durrant, *J. Am. Chem. Soc.* **2004**, *126*, 5225–5233; c) J.-H. Yum, P. Chen, M. Grätzel, M. K. Nazeeruddin, *ChemSusChem* **2008**, *1*, 699–707; d) A. Kay, M. Graetzel, *J. Phys. Chem.* **1993**, *97*, 6272–6277; e) K. Hara, Y. Dan-oh, C. Kasada, Y. Ohga, A. Shinpo, S. Suga, K. Sayama, H. Arakawa, *Langmuir* **2004**, *20*, 4205–4210.
- [7] J. Yang, P. Ganesan, J. Teuscher, T. Moehl, Y. J. Kim, C. Yi, P. Comte, K. Pei, T. W. Holcombe, M. K. Nazeeruddin, et al., *J. Am. Chem. Soc.* **2014**, *136*, 5722–5730.
- [8] a) S. S. Park, Y. S. Won, Y. C. Choi, J. H. Kim, *Energy Fuels* **2009**, *23*, 3732–3736; b) C.-H. Yang, S.-H. Liao, Y.-K. Sun, Y.-Y. Chuang, T.-L. Wang, Y.-T. Shieh, W.-C. Lin, *J. Phys. Chem. C* **2010**, *114*, 21786–21794; c) X. Jiang,

- K. M. Karlsson, E. Gabriellsson, E. M. J. Johansson, M. Quintana, M. Karlsson, L. Sun, G. Boschloo, A. Hagfeldt, *Adv. Funct. Mater.* **2011**, *21*, 2944–2952; d) S. Ramkumar, S. Manoharan, S. Anandan, *Dye. Pigment.* **2012**, *94*, 503–511; e) M. S. Kim, H. S. Yang, D. Y. Jung, Y. S. Han, J. H. Kim, *Colloids Surf. A* **2013**, *420*, 22–29; f) G. Paramaguru, N. Nagarajan, R. Renganathan, *J. Mol. Struct.* **2013**, *1038*, 235–241; g) Y. Ooyama, N. Yamaguchi, I. Imae, K. Komaguchi, J. Ohshita, Y. Harima, *Chem. Commun.* **2013**, *49*, 2548–2550; h) W.-I. Hung, Y.-Y. Liao, C.-Y. Hsu, H.-H. Chou, T.-H. Lee, W.-S. Kao, J. T. Lin, *Chem. Asian J.* **2014**, *9*, 357–366; i) W. Lee, S. B. Yuk, J. Choi, H. J. Kim, H. W. Kim, S. H. Kim, B. Kim, M. J. Ko, J. P. Kim, *Dye. Pigment.* **2014**, *102*, 13–21.
- [9] a) H. Zhang, J. Fan, Z. Iqbal, D.-B. Kuang, L. Wang, H. Meier, D. Cao, *Org. Electron.* **2013**, *14*, 2071–2081; b) K. S. V. Gupta, T. Suresh, S. P. Singh, A. Islam, L. Han, M. Chandrasekharan, *Org. Electron.* **2014**, *15*, 266–275; c) H.-C. Chu, D. Sahu, Y.-C. Hsu, H. Padhy, D. Patra, J.-T. Lin, D. Bhattacharya, K.-L. Lu, K.-H. Wei, H.-C. Lin, *Dye. Pigment.* **2012**, *93*, 1488–1497; d) R. Grisorio, L. De Marco, G. Allegretta, R. Giannuzzi, G. P. Suranna, M. Manca, P. Mastrolilli, G. Gigli, *Dye. Pigment.* **2013**, *98*, 221–231; e) G. D. Sharma, J. A. Mikroyannidis, M. S. Roy, K. R. J. Thomas, R. J. Ball, R. Kurchania, *RSC Adv.* **2012**, *2*, 11457–11464; f) V. Leandri, R. Ruffo, V. Trifiletti, A. Abboto, *Eur. J. Org. Chem.* **2013**, *2013*, 6793–6801; g) C. Y. Lee, C. She, N. C. Jeong, J. T. Hupp, *Chem. Commun.* **2010**, *46*, 6090–6092; h) L. Yu, J. Xi, H. T. Chan, T. Su, L. J. Antrobus, B. Tong, Y. Dong, W. K. Chan, D. L. Phillips, *J. Phys. Chem. C* **2013**, *117*, 2041–2052; i) Y. S. Yang, H. Do Kim, J.-H. Ryu, K. K. Kim, S. S. Park, K.-S. Ahn, J. H. Kim, *Synth. Met.* **2011**, *161*, 850–855.
- [10] a) X. Ren, S. Jiang, M. Cha, G. Zhou, Z.-S. Wang, *Chem. Mater.* **2012**, *24*, 3493–3499; b) K. D. Seo, B. S. You, I. T. Choi, M. J. Ju, M. You, H. S. Kang, H. K. Kim, *Dye. Pigment.* **2013**, *99*, 599–606; c) D. Cao, J. Peng, Y. Hong, X. Fang, L. Wang, H. Meier, *Org. Lett.* **2011**, *13*, 1610–1613; d) Y. Hong, J.-Y. Liao, J. Fu, D.-B. Kuang, H. Meier, C.-Y. Su, D. Cao, *Dye. Pigment.* **2012**, *94*, 481–489.
- [11] N. Manfredi, B. Cecconi, A. Abboto, *Eur. J. Org. Chem.* **2014**, *2014*, 7069–7086.
- [12] a) B. Zietz, E. Gabriellsson, V. Johansson, A. M. El-Zohry, L. Sun, L. Kloo, *Phys. Chem. Chem. Phys.* **2014**, *16*, 2251–2255; b) C. Chen, X. Yang, M. Cheng, F. Zhang, L. Sun, *ChemSusChem* **2013**, *6*, 1270–1275.
- [13] P. Ganesan, A. Chandiran, P. Gao, R. Rajalingam, M. Grätzel, M. K. Nazeeruddin, *J. Phys. Chem. C* **2014**, *118*, 16896–16903.
- [14] P. Gao, Y. J. Kim, J.-H. Yum, T. W. Holcombe, M. K. Nazeeruddin, M. Grätzel, *J. Mater. Chem. A* **2013**, *1*, 5535–5544.
- [15] A. Bard, L. Faulkner, *Electrochemical Methods: Fundamentals and Applications*, Wiley, New York, **2001**.
- [16] Z.-S. Wang, K. Hara, Y. Dan-oh, C. Kasada, A. Shinpo, S. Suga, H. Arakawa, H. Sugihara, *J. Phys. Chem. B* **2005**, *109*, 3907–3914.
- [17] A. Kira, Y. Matsubara, H. Iijima, T. Umeyama, Y. Matano, S. Ito, M. Niemi, N. V. Tkachenko, H. Lemmetyinen, H. Imahori, *J. Phys. Chem. C* **2010**, *114*, 11293–11304.
- [18] J. Wiberg, T. Marinado, D. P. Hagberg, L. Sun, A. Hagfeldt, B. Albinsson, *J. Phys. Chem. C* **2009**, *113*, 3881–3886.

Received: November 20, 2014

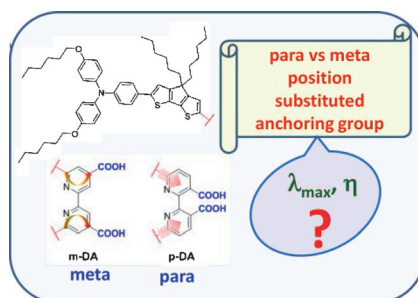
Published online on ■ ■ ■, 2015

## ARTICLES

P. Ganesan, A. K. Chandiran, P. Gao,\*  
R. Rajalingam, M. Grätzel,  
M. K. Nazeeruddin\*

■■■ - ■■■

Double D- $\pi$ -A Dye Linked by 2,2'-Bipyridine Dicarboxylic Acid: Influence of *para*- and *meta*-Substituted Carboxyl Anchoring Group



**On the bench:** Two new (D- $\pi$ -A)<sub>2</sub> organic sensitizers (*m*-DA, *p*-DA) employing a 2,2'-bipyridine dicarboxylic acid unit as an acceptor and anchoring group are designed. The *m*-DA has the anchoring part substituted *meta* to the donor moiety and *p*-DA has a *para*-substituted anchoring moiety. Overall, *para*-substituted *p*-DA exhibits better photovoltaic performance than *meta*-substituted *m*-DA.